Amphiphilic polymers bearing gluconolactone moieties: Synthesis and long side-chain crystalline behavior

María L. Cerrada[a], Vanesa Bordegé[a], Alexandra Muñoz-Bonilla[a], Orietta León[a], Rocío Cuervo-Rodríguez[b], Manuel Sánchez-Chaves[a], Marta Fernández-García[a],[*]

[a] Instituto de Ciencia y Tecnología de Polímeros (ICTP-CSIC), C/ Juan de la Cierva 3, 28006 Madrid, Spain
[b] Facultad de Ciencias Químicas, Universidad Complutense de Madrid, Av. Complutense s/n, Ciudad Universitaria, 28040 Madrid, Spain

ARTICLE INFO

ABSTRACT

The synthesis and characterization of amphiphilic polymers bearing gluconolactone moieties has been described. In a first step, an unprotected glycomonomer 2-[({[4-(D-gluconamid-N-yl)butyl]amino}carbonyl)oxy]ethyl acrylate, HEAG, has been synthesized. Posterior, this glycomonomer has been copolymerized with methyl methacrylate at different compositions and the kinetic behavior has been also studied calculating the monomer reactivity ratios by Kelen–Tüdös extended equation. In addition, the long side-chain crystalline behavior of these carbohydrate-based copolymers with high composition of glycomonomer has been examined by using conventional and modulated differential scanning calorimetry and X-ray diffraction measurements. At the same time, the phase separation behavior of carbohydrate-based copolymers with lower HEAG content has been determined by their glass transition temperature measurements. Finally, the thermal stability of all these amphiphilic copolymers has been evaluated by thermogravimetric analysis.

© 2013 Elsevier Ltd. All rights reserved.

1. Introduction

Synthetic polymers bearing carbohydrate groups in the side chain or at the end of the macromolecular chain (also known as glycopolymers) have become a hot topic for investigation within the scientific community and attracted great interest because of their potential applications in biomedicine and biomaterials (Okada, 2001; Varma, Kennedy, & Galgali, 2004). In particular, carbohydrate-based polymers containing cyclic saccharides potentiate multivalent protein–carbohydrate interactions in living organisms, which lead to biomolecular recognition events that are dramatically different from those elicited by monovalent interactions (Bertozzi & Kiessling, 2001; Kiessling, Gestwicki, & Strong, 2006; Mammen, Choi, & Whitesides, 1998) Much research has been focused on hydrogels (Chen, Dordick, & Rethwisch, 1995; Zhou, Kurth, Hsieh, & Krochta, 1999) cell culture substrates (Bahulekar et al., 1998) artificial organs (Karamuk, Mayer, Wintermantel, & Akaike, 1999) lectin recognition materials (Bertozzi & Kiessling, 2001; García-Oteiza, Sánchez-Chaves, & Arranz, 1997; Kobayashi, Tsuchida, Usui, & Akaike, 1997; Ting, Chen, & Stenzel, 2010) and drug delivery systems (Polikarpov, Kaufmann, Kluge, Appelhans, &

Voit, 2010; Top & Kiick, 2010). Also, these carbohydrate polymers are potential surface modifiers for the development of interfacial properties to meet the requirements of biomedical uses. In contrast, saccharides with open-chain structures are more efficient than those with cyclic ones (Okada, 2001) in improving the hydrophilicity of the polymeric material surface. This increase in hydrophilicity at surface favors undesirable adhesion of proteins, cells, or other molecules (Bordege et al., 2011; Ting et al., 2010; Xu, Wan, & Huang, 2009; Yang, Xu, Dai, Wang, & Ulbricht, 2005) and promotes a characteristic as important as hemocompatibility.

In some cases carbohydrate polymers can be then considered as grafted amphiphilic chemical architectures because of their pendant carbohydrate moieties linked to the backbone. Graft copolymers, as well as the block ones, have been recognized as advanced nanomaterials because they can self-assemble into various ordered patterns (spheres, cylinders, lamellae, or bicontinuous double diamonds) in the condensed state and in solution depending, basically, on the volume fraction of each component, the difference in their solubility parameters, sample preparation, and thermal history (de la Fuente, Fernandez-Garcia, Cerrada, Spiess, & Wilhelm, 2006; Hadjichristidis, Pispas, & Floudas, 2003; Lee et al., 1997; Matsushita & Noda, 1996; Munoz-Bonilla, Cerrada, & Fernandez-Garcia, 2007a, 2007b; Munoz-Bonilla, Fernandez-Garcia, Cerrada, Mantovani, & Haddleton, 2007; Munoz-Bonilla, Fernandez-Garcia, & Haddleton, 2007; Muñoz-Bonilla et al., 2012)

---

* Corresponding author. Tel.: +34 912587505; fax: +34 915644853.
  E-mail address: martafg@ictp.csic.es (M. Fernández-García).

This self-assembly capability, sometimes called nanophase separation (Chen & Wunderlich, 1999) is observed in X-ray scattering measurements by characteristic "peaks" at scattering vector scale in the range $0.2 \leq q \leq 0.6\,\text{Å}^{-1}$. Moreover, carbohydrate copolymers, mainly those with open-chain structure, could be able of exhibiting side-chain crystallization if their pendant chains are long enough. Nevertheless, to the best of our knowledge, no examples of extensive studies about synthetic semi-crystalline carbohydrate polymers have been reported. Crystallization behavior of polymers containing long *n*-alkyl groups in the side chain has been analyzed in the past decades by various groups focusing on different aspects (Beiner, 2001; Cowie, Haq, McEwen, & Veličković, 1981; Jones, 1964; Jordan, 1971; Jordan, Artymyshyn, Speca, & Wrigley, 1971; Karaky, Clisson, Reiter, & Billon, 2008; López-Velázquez, Bello, & Pérez, 2004; McKenzie, Nudelman, Bomans, Holder, & Sommerdijk, 2010; Mogri & Paul, 2001a, 2001b; Neugebauer, Theis, Pakula, Wegner, & Matyjaszewski, 2005; O'Leary & Paul, 2006; Pankaj, Hempel, & Beiner, 2009). This capability of organizing at short range into three-dimensional crystallites confers a very interesting feature since the whole properties array will depend on the crystalline morphology. Accordingly, variations on crystallization conditions, which might lead primarily to changes in degree of crystallinity and crystallite size, would allow tuning specific requirements and, thus, designing "smart" materials exhibiting desirable complex responses.

The synthesis of carbohydrate-containing polymers with well-defined structure is usually performed by two methods (Cameron et al., 2008; Gauthier, Gibson, & Klok, 2009; Ladmiral, Melia, & Haddleton, 2004; Okada, 2001; Spain & Cameron, 2011; Spain, Gibson, & Cameron, 2007; Ting et al., 2010; Varma et al., 2004): (a) the polymerization or copolymerization of carbohydrate-bearing monomers by conventional or controlled polymerization techniques; and (b) the chemical modification of a reactive polymer scaffold with carbohydrates. In these two methodologies, the saccharide is attached to the polymer by ester, amide, carbamate, ether linkages among others. It is important to avoid, if possible, undesirable sugar protecting/deprotecting processes because these multi-step reactions make tedious the synthetic protocol in addition to reduce their overall yield.

This investigation is focused on the synthesis of several glycopolymers based on methyl methacrylate, MMA, and 2-[({[4-(D-gluconamid-N-yl)butyl]amino}carbonyl)oxy]ethyl acrylate, HEAG, an unprotected glycomonomer. Classical free radical polymerization has been chosen as synthetic methodology in this investigation since, on one hand, it is a versatile, robust and the most industrially used protocol and, on the other hand, because the preparation of these proposed novel and very interesting amphiphilic carbohydrate copolymers is feasible in rather mild conditions without further requirements of protecting/deprotecting processes. In addition, copolymerization reactions have been thoroughly studied and their kinetic, copolymer composition variation and monomer reactivity ratios have been determined.

A major field of applicability for carbohydrate based copolymers is related to their potential capability for protein binding in water solutions. Other properties, different than those evaluated in solution, should be, however, explored in order to seek other high-added-value applications, replacing the existing materials and allowing also new markets to be created. A very important aspect is, then, to learn how these carbohydrate polymeric chains are organized at molecular level in the solid state which allow us to interpret changes in their physical properties. Accordingly, determination of the phase transitions and thermal stability becomes an important issue in these copolymers that are used, for instance, in pharmaceutical products in order to perform a proper handling, manufacturing and storage conditions of these materials. To assess this additional target, phase transitions have been analyzed by

X-ray diffraction measurements at small and wide angles using synchrotron and conventional radiation, respectively, as well as by conventional and modulated differential scanning calorimetry, DSC and MDSC, experiments; and, the thermal stability of the resultant carbohydrate copolymers has been checked by thermogravimetry, TGA.

2. Experimental

2.1. Materials

2-Hydroxyethyl acrylate, HEA (Fluka, 99%) and methyl methacrylate, MMA (Merck), were purified by a conventional method (Stickler, 1987) 2,2′-Azobisisobutyronitrile, AIBN (Fluka), was purified by successive crystallizations from methanol. *p*-Nitrophenyl chloroformate (Fluka, 97%), glucono-1,5 lactone (99%, Fluka) and 1,4-diaminobutane (Fluka) were used without further purification. Dimethyl sulfoxide, DMSO (Scharlau), and triethylamine (Scharlau) were previously distilled; methanol (Fluka), ether dioxide (SDS), and ethanol (Normapur) were used as received.

2.2. Synthesis of glycomonomer, HEAG

The aminosaccharide, N-(4-aminobutyl)-D-gluconamide, NABG (Cerrada, Sanchez-Chaves, Ruiz, & Fernandez-Garcia, 2009) and activated HEA with *p*-nitrophenyl chloroformate, HEAN (Bordegé et al., 2011) were prepared as described in literature. Then, the glycomonomer, 2-[({[4-(D-gluconamid-N-yl)butyl]amino}carbonyl)oxy]ethyl acrylate, HEAG, was synthesized as follows (see Scheme 1):

N-(4-aminobutyl)-D-gluconamide (4.75 g, 17.8 mmoles) with hydroquinone (0.01 g) solved in DMSO (20 mL) was slowly added at 30 °C to a DMSO solution (20 mL) of HEAN (5.02 g, 17.8 mmoles). The mixture was stirred for 2 h and afterwards, it was precipitated into a large excess of dichloromethane. The product was filtered and washed with acetone giving a white solid, HEAG glycomonomer (6.59 g, 91%). The ^{1}H and ^{13}C NMR spectra are shown in Fig. S1 of Supporting Information.

2.3. Polymerization reaction

The monomers were polymerized with AIBN as initiator (3×10^{-2} mol/L) and with DMSO as solvent (1 mol/L) at 70 ± 0.5 °C. The copolymerization was monitored by in situ ^{1}H NMR measurements using a tube sealed under argon atmosphere. These copolymers were also obtained at high conversions using Pyrex glass ampoules sealed under argon atmosphere in a thermostatic bath at 70 ± 0.1 °C. The carbohydrate copolymers purification was performed by dialysis using a membrane of 3500 Daltons (Cellu Sep T1) and posterior lyophilization in a Telstar Lioalfa-6.

The carbohydrate based statistical copolymers performed at total conversion have been labeled as P(M*x*G*y*), *x* and *y* referring the MMA and HEAG molar fraction in the copolymer, respectively.

2.4. Nuclear magnetic resonance spectroscopy (NMR)

Proton spectra, ^{1}H NMR, were recorded using a Varian Inova-400 spectrometer operating at 400 MHz in DMSO-d_6 solutions (25%, w/v) at 70 °C. The spectra parameters were: acquisition time 3.7 s, pulse of 7.0 μs, 128 runs and without delayed time. The delayed time variation (2, 5, 10 s) and/or pulse width do not imply a significant change in the signals.
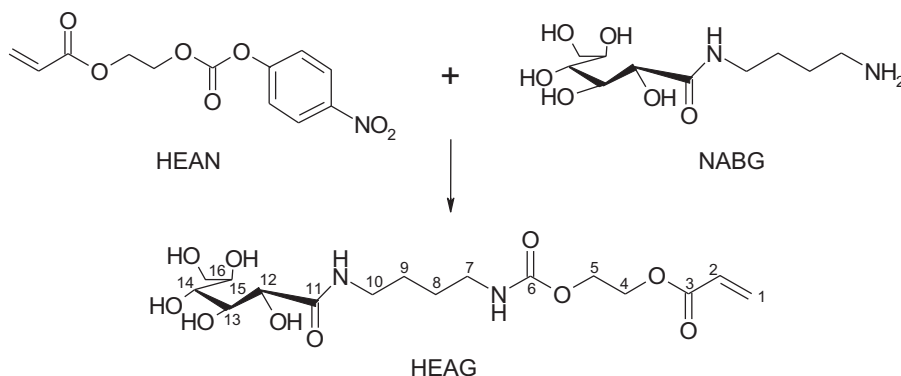
Scheme 1. Synthesis of HEAG monomer.

2.5. Wide-angle X-ray diffraction (WAXS)

WAXS experiments were carried out using a Bruker D8 Advance diffractometer with a Ni-filtered Cu K_α radiation ($\lambda = 1.54$ Å). The samples were heated from 30 to 160 °C at intervals of 5 °C and the corresponding diffraction scans were collected at a rate of 0.1°/s, between 2θ values from 4° to 32°. The goniometer was calibrated with a standard of silicon. The estimated error was ±0.2°.

2.6. Small angle X-ray diffraction (SAXS)

SAXS measurements with X-ray synchrotron radiation were performed in the soft-condensed matter beamline A2 at Hasylab (Hamburg, Germany), working at a wavelength of 1.50 Å. The experimental setup included a specimen holder and a MARCCD detector for acquiring two-dimensional SAXS patterns (sample-to-detector distance being 260 cm). The different orders of the long spacing of rat-tail cornea ($L = 65$ nm) were utilized for calibration of the SAXS detector. The 2D X-ray diffractograms were processed using the A2tool program developed to support beamline A2 data processing. The profiles were normalized to the primary beam intensity and the background from an empty sample was subtracted. All experiments comprise the heating of samples from 28 up to 160 °C at 8 °C/min. The data acquisition was done in frames of 15 s.

2.7. Differential scanning calorimetry (DSC)

Conventional and modulated differential scanning calorimetric measurements were performed in a TA Instruments, DSC Q100 equipment, with an Intracooler for low temperatures. The temperature scale was calibrated from the melting point of high purity indium. Samples (∼3–5 mg) weighed with an electronic autobalance (Perkin-Elmer AD4), were scanned at 10 °C/min under dry nitrogen (50 cm³/min). The conventional experiments consisted of a first heating run from −40 °C to 160 °C, after cooling down from room temperature to −40 °C. Subsequently to this first heating process, samples were then cooled down to −40 °C at the same rate, and then a new successive heating run was performed.

Furthermore, MDSC experiments were performed with a sinusoidal temperature oscillation overlaid on the linear temperature ramp. Preferred modulation parameters were a period of 40 s, a modulation amplitude of ±0.531 °C and an underlying heating rate of 5 °C/min. Identical temperature range, from −40 °C to 160 °C, was evaluated.

The actual value for the glass transition temperature, T_g, was estimated as the temperature at the midpoint of the line drawn between the temperature of intersection of the initial tangent with the tangent drawn through the point of inflection of the trace and the temperature of intersection of the tangent drawn through the point of inflection with the final tangent. The quoted value is the average of several measurements on each sample.

2.8. Thermal stability

The thermogravimetric measurements were performed in a TA Instruments, TGA Q500 equipment. The instrument was calibrated both for temperature and weight by standard methods. Non-isothermal experiments were performed in the temperature range 40–700 °C at heating rate of 10 °C/min. The average sample size was ca. 5 mg and the dry nitrogen flow rate was 20 cm³/min.

3. Results and discussion

3.1. Copolymerization reactions

Copolymerization reactions were carried out in DMSO-d_6 solutions at 70 °C using a total monomers concentration of 1 M and an AIBN initiator concentration of 3×10^{-2} M (see Scheme 2) in NMR glass tubes under argon atmosphere.

The initial feed molar fractions were 0.1, 0.3, 0.5, 0.7 and 0.9. All these reactions were monitored by in situ ¹H NMR considering the variation of double bond signals of both monomers through the reaction, as shown in Fig. S2 for the system with a HEAG feed molar fraction of 0.3. The peaks at 5.7 and 6.0 ppm correspond to the two protons of MMA vinyl double bond while those at 5.9, 6.1 and 6.3 ppm are ascribed to the three protons of the HEAG comonomer.

The individual conversion of each comonomer as a function of copolymerization time for each initial molar fraction in the feed is easily calculated from the ¹H NMR spectra (see Fig. S3). It is clearly noticeable that MMA comonomer is firstly consumed independently of the HEAG molar fraction in the feed.

The rate of copolymerization can be expressed as

$$R_p = -\frac{d[M]}{dt} = \frac{\overline{k_p}}{k_t^{1/2}}(2fk_d[I])^{1/2}[M] \tag{1}$$

where f and k_d are the efficiency factor and the kinetic coefficient for the initiation reaction; k_p and k_t are the kinetic coefficients for propagation and termination, respectively; and $[I]$ and $[M]$ are the initiator and global monomer concentrations, respectively. Eq. (1) can also be written as

$$\ln\left(\frac{1}{1-x}\right) = \frac{\overline{k_p}}{k_t^{1/2}}(2fk_d[I])^{1/2}t = K_{\exp}t \tag{2}$$

where $x = ([M]_0 - [M])/[M]_0$ is the global conversion.
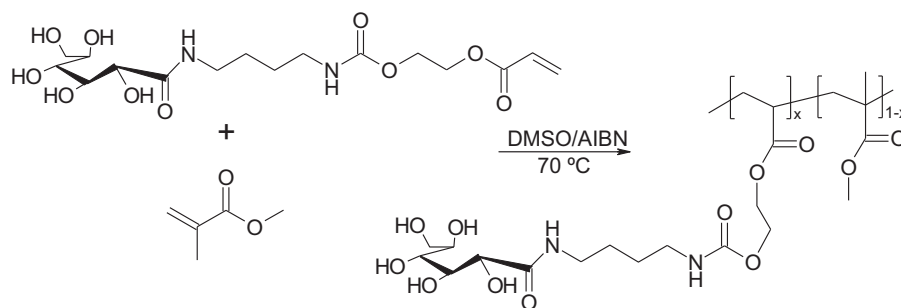
Scheme 2. Copolymerization reaction of HEAG and MMA.

Fig. 1a displays the linear part of $\ln(1/(1-x))$ representation against time. An increase of copolymerization rate is observed as HEAG molar fraction in the feed is raised. The copolymerization global constants, $(\overline{k_p/k_t^{1/2}})(2fk_d)^{1/2}$, are estimated from the corresponding slopes. An almost linear dependence on HEAG molar fraction in the feed is shown as depicted in Fig. 1b. The obtained data are also collected in Table S1.

The HEAG molar fraction in the feed and in the copolymer throughout conversion is also obtained from ^{1}H NMR data. Fig. 2 shows the corresponding experimental results at each molar fraction used in the feed. As can be seen, both feed and copolymer molar fractions increase with HEAG glycomonomer composition in the system.
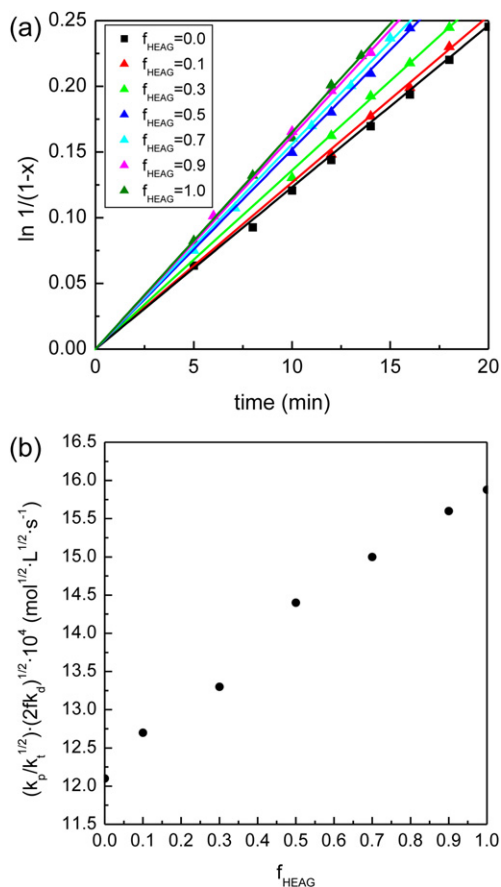
The monomer reactivity ratios were calculated using the Kelen–Tüdös extended equation (Tudos, Kelen, Foldesberezsnich, & Turcsanyi, 1976)

$$F = \frac{F_1/F_2}{[(\log z_1)/(\log z_2)]^2} \tag{3}$$

$$G = \frac{(F_1/F_2) - 1}{[(\log z_1)/(\log z_2)]^2} \tag{4}$$

$$G = r_1 F - r_2 \tag{5}$$

where r_i and F_i are the i monomer reactivity ratio and cumulative molar fraction of i monomer in the copolymer, respectively, and $z_i = f_{i,0}/f_{i,f}$ where $f_{i,0}$ and $f_{i,f}$ are initial and final mole fractions of i
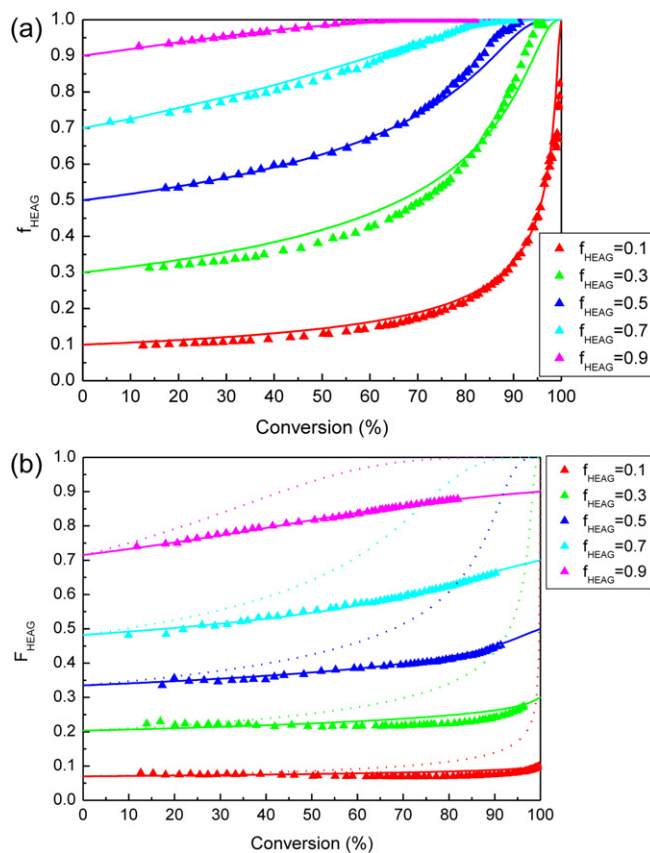

Fig. 1. (a) Linear part of representation of $\ln 1/(1-x)$ against time for each initial molar fraction in the feed; (b) copolymerization global constants variation as a function of HEAG initial molar fraction in the feed, f_{HEAG}.

Fig. 2. Variation of cumulative (a) feed, f_{HEAG}, and (b) copolymer, F_{HEAG}, molar fractions as a function of conversion for each initial feed molar fraction in the carbohydrate copolymer.

monomer, respectively. Eq. (5) can be transformed by introducing new variables, η and ε and a symmetric parameter α:

$$\eta = \left(r_1 + \frac{r_2}{\alpha} \right) \varepsilon - \frac{r_2}{\alpha} \qquad (6)$$

where the variables are defined as $\eta = G/(\alpha + F)$ and $\varepsilon = F/(\alpha + F)$, and the parameter α is expressed as $(F_{max} \cdot F_{min})^{0.5}$. Fig. S4 displays this equation for the statistical copolymers with conversions ranging from 20 to 50% following the recommendations of Kelen and co-workers (Tudos et al., 1976). The results obtained are $r_{HEAG} = 0.21 \pm 0.03$ and $r_{MMA} = 1.40 \pm 0.02$, indicating that the reactivity of MMA radical against HEAG is lower than against MMA, whereas HEAG radical reacts rather with MMA than with its gly-comonomer.

It is important to mention that the copolymerization Mayo–Lewis Terminal Model (Mayo & Lewis, 1944) can be used for descriptive purposes (Fukuda, Goto, Kwak, Yoshikawa, & Ma, 2002) although it is only an approximate model (Coote & Davis, 1999). Therefore, to evaluate the estimated monomer reactivity ratios, the cumulative feed and copolymer molar fractions as a function of conversion for the different initial compositions in the feed are compared with the theoretically calculated values. The solid lines of Fig. 2 are drawn according to the integrated copolymer composition equation with the monomer reactivity ratios previously calculated. As can be easily noticed, a good agreement between the experimental and calculated data is found. The instantaneous copolymer compositions, which are defined as:

$$F_{1,inst} = \left(\frac{r_1 f_1^2 + f_1 f_2}{r_1 f_1^2 + r_2 f_2^2 + 2 f_1 f_2} \right) \qquad (7)$$

are also included as dotted lines in Fig. 2b at each molar fraction. Their variation gives an idea of the relative change in monomer composition. As can be seen, MMA is completely consumed exclusively at elevated HEAG molar fraction in the feed and high conversions (>80–90%), and, then, a small proportion of HEAG homopolymer exists. Therefore, properties of these glycopolymers should be those resultant ones of having randomly formed copolymers.

To analyze these physico-chemical properties exhibited by the copolymers, reactions were carried out at very high conversion degrees in DMSO solutions using a total monomers concentration of 1 M and an AIBN initiator concentration of 3×10^{-2} M in Pyrex glass ampoules sealed under argon atmosphere in thermostatic bath at $70 \pm 0.1\,^\circ$C. In this case, the initial feed molar fractions were ranging from 0.1 to 0.9. Since the copolymers are practically performed up to total conversion, their copolymer compositions are practically the same to the initial feed ones, $f_{initial,HEAG} \cong F_{final,HEAG}$ (see Fig. 2). The carbohydrate copolymer purification was also performed by dialysis.

3.2. Characterization of crystalline and amorphous details

Fig. 3a displays the conventional DSC traces during the first heating run for PMMA and PHEAG polymers. PMMA is an amorphous polymer and, then, exhibits exclusively a thermal transition on heating, i.e., the glass transition (T_g^{MMA}). It is located at ca. 100.0 °C similar to those values reported in the literature (Feijoo, Muller, & Acosta, 1986; Fernandez-Garcia, Cuervo-Rodriguez, & Madruga, 1999; Fernandez-Garcia, Lopez-Gonzalez, Barrales-Rienda, Madruga, & Arias, 1994; Teng et al., 2009). The PHEAG shows several thermal transitions on the heating run. It can be observed in order of increasing temperatures: the glass transition (T_g^{HEAG}) that appears at around 16 °C, a small endothermic process taking place at about 70 °C and a primary endothermic transition whose peak occurs at approximately 140 °C. The presence of these processes indicates the semicrystalline nature of this
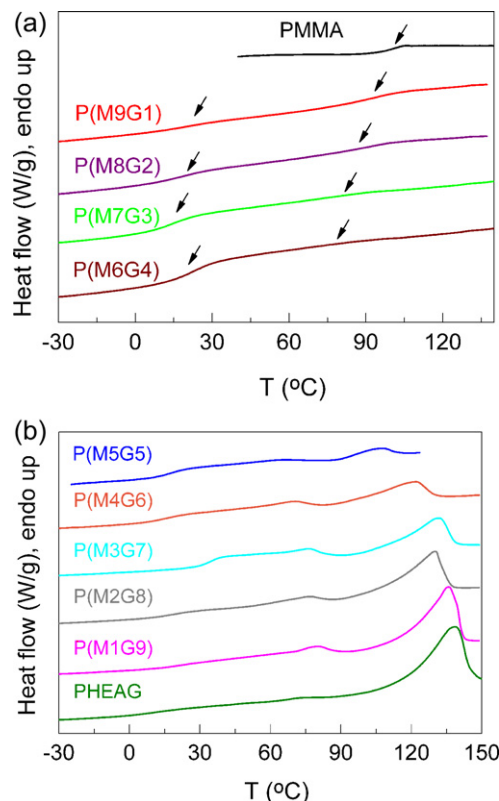

Fig. 3. DSC first heating thermograms: (a) PMMA and PHEAG; (b) PMMA and carbohydrate copolymers with $F_{HEAG} < 0.5$; (c) PHEAG and carbohydrate copolymers with $F_{HEAG} \geq 0.5$.

carbohydrate polymer. Additionally, it should be commented that although the PHEAG has a diaminobutyl flexible spacer as well as an open-ring carbohydrate within the lateral chain, its T_g^{HEAG} temperature is similar to that found in its PHEA precursor (Gómez Tejedor, Rodríguez Hernández, Gómez Ribelles, & Monleón Pradas, 2007; Mun et al., 2004) i.e., 15–20 °C. This fact is attributed to the strong inter and intramolecular interactions between carbohydrate hydroxyl groups, which reduce the chain mobility and increase polymer rigidity.

This semicrystalline nature is preserved in some of P(MxGy) copolymers. In fact, some ordering is even developed in the P(M5G5) copolymer although it is rather deficient, as deduced from its WAXS profile at room temperature depicted in Fig. 4a. Those copolymers with F_{HEAG} values lower than 0.5 are completely amorphous, as it is noticeably observed in Fig. 3b. They show, however, two glass transitions: one located in the closeness, but at lower temperature, of that ascribed to the PMMA homopolymer and the other one taking place in the proximity of the T_g associated with the cooperative motions within the PHEAG chains, although at slightly higher temperature (see values in Table S2).

This feature could be considered unforeseen because of the statistical distribution of both counits within the copolymer. Nevertheless, it might be attributed to their amphiphilic character and the appropriate length of these two, methacrylic and saccharide-containing, segments within the composition range that boost an almost complete phase separation. To this respect each phase is characterized by its own and individual generalized segmental movements: the one related to the long side chains of carbohydrate co-units and that corresponding to the backbone, appearing at low and high temperature, respectively. It is noteworthy that the T_g dependence on composition, within this interval, is in that associated with the lateral chains (T_g^1) much less important than
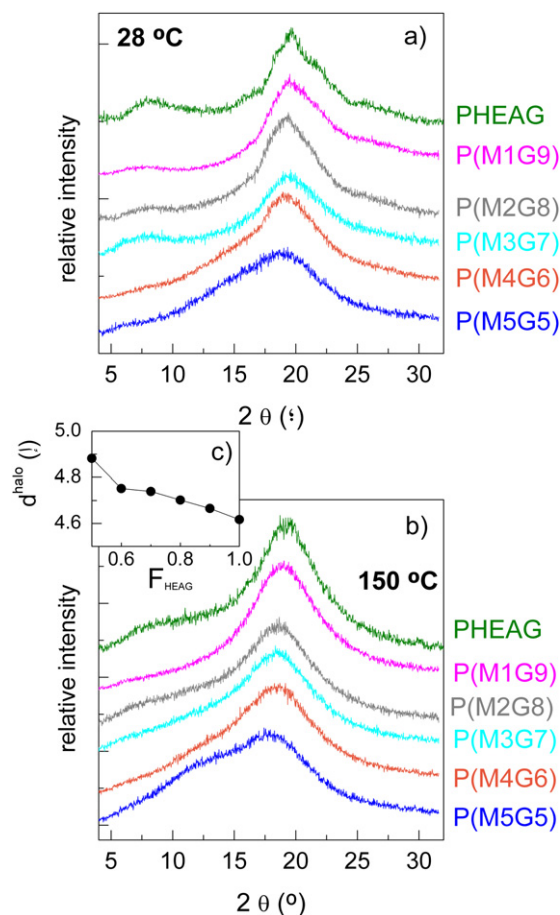
Fig. 4. Wide-angle X-ray profiles: (a) at 28 °C; (b) at 150 °C; (c) spacing values at 150 °C of amorphous halo at the different HEAG compositions.

that ascribed to the backbone (T_g^2). Incorporation of saccharide side chains breaks up chemical regularity of methacrylic main chain and, then, the steric hindrance promoted by its methyl and ester groups responsible of its T_g at around 100 °C is minimized. Accordingly, an important shift of T_g^2 to lower temperatures is seen as lateral carbohydrated content increases.

Additional MDSC experiments have been performed to confirm the existence of these two glass transition processes. The normal temperature scan used in DSC is, generally, overlaid by a sinusoidal perturbation in the MDSC technique. The purported advantages of MDSC include the ability to separate overlapping phenomena, as well as improved resolution and sensitivity. The modulated heat flow raw data are deconvoluted by Fourier Transform algorithm (Wunderlich, 1997) allowing calculation in MDSC experiments of the reversing heat flow (caused by modulation) and the total heat flow (caused by the underlying heating rate, which corresponds to conventional DSC data). The difference is the non-reversing heat flow, which takes into consideration the contribution of all the kinetics events that cannot follow the modulation. It has been empirically found that: (1) the glass transition appears in the total and reversing component of the heat flow; (2) the crystallization process is observed in the total and non-reversing component, but not in the reversing component of the heat flow; and (3) the melting process may be visible in all three components of the resolved data (Höhne, 1999; Reading, Luget, & Wilson, 1994; Simon, 2001; Wunderlich et al., 1999). Fig. 5a shows the results found for total heat flow as well as its reversing and non-reversing components in the P(M8G2) carbohydrate copolymer. The overall heat flow is rather analogous to that obtained from the conventional DSC
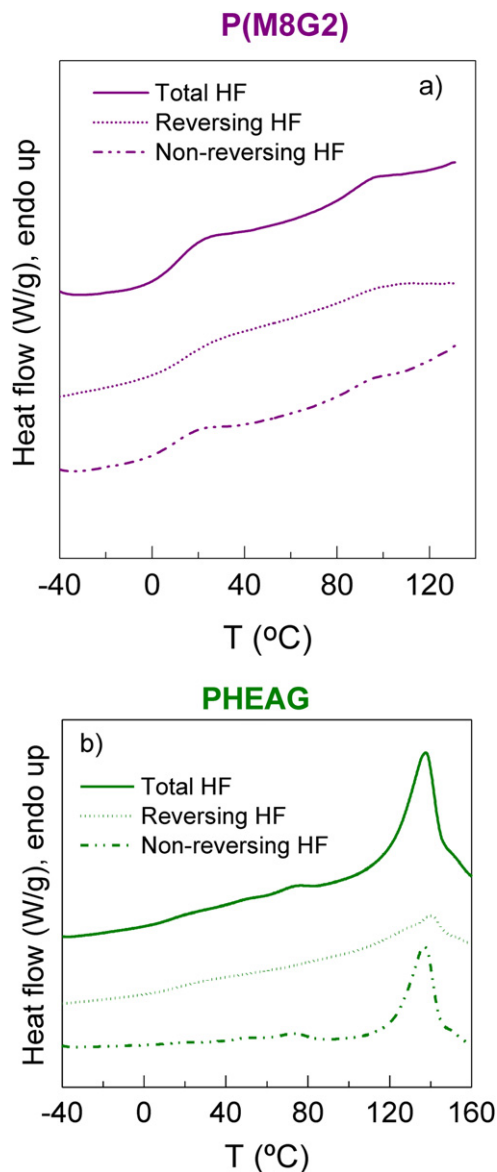

Fig. 5. MDSC curves (total, reversing and non-reversing heat flow, HF), obtained during the first heating process for (a) P(M8G2) and (b) PHEAG carbohydrate polymers.

experiments and the two glass transitions processes are clearly seen in the reversing response. They are located at 19.5 °C and 92.0 °C for T_g^1 and T_g^2, respectively, being in a good agreement with the results attained by conventional DSC. Low intense enthalpy relaxation processes are overlapped to these glass transitions related to the cooperative segmental motions existing in this P(M8G2) copolymer.

Fig. 3c shows the phase transitions exhibited by the rest of the carbohydrate copolymers, i.e., those with HEAG molar fractions in the copolymer equal or higher than 0.5. Similar behavior to that presented by PHEAG is clearly observed. In order of increasing temperatures, the glass transition appears followed by a small endothermic process and a primary endothermic peak. These three thermal events are also seen in the MDSC response as represented in Fig. 5b for PHEAG homopolymer. The T_g and a fraction of the main melting process appear in the reversing component while the small endotherm placed at low temperature and the rest of the primary melting process is detected in the non-reversing response. An obvious dependence upon F_{HEAG} is observed for the intensity
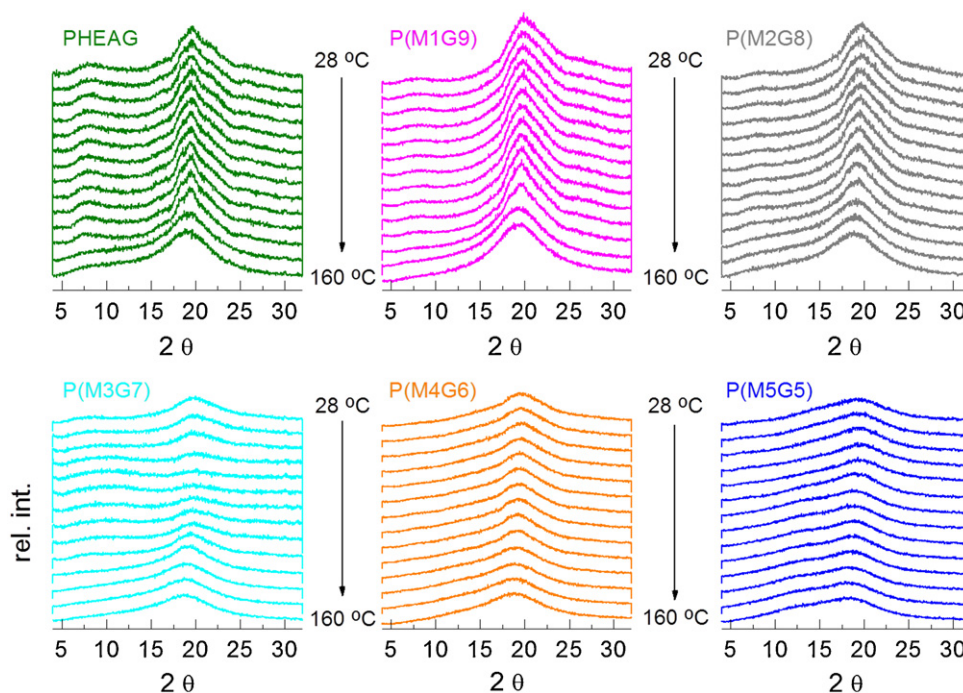
Fig. 6. Variable-temperature wide-angle X-ray patterns for P(M*x*G*y*) copolymers with HEAG compositions equal or higher than 0.5.

and location of the primary melting process. An increase, now, of the methacrylic comonomer interrupts the self-assembly capability of lateral saccharide-containing chains in organized entities. Consequently, the ordered domains become less in amount and in perfection leading to a decrease in intensity and a very significant melting point depression as MMA content is raised in the carbohydrate copolymer.

Fig. 4 corroborates, as aforementioned, the existence of ordering in these copolymers with HEAG compositions equal or higher than 0.5, showing the WAXS profiles at room temperature (Fig. 4a) and those obtained once their isotropic state has been reached (Fig. 4b). As commented above (Beiner, 2001; Cowie et al., 1981; Jones, 1964; Jordan, 1971; Jordan et al., 1971; Karaky et al., 2008; López-Velázquez et al., 2004; McKenzie et al., 2010; Mogri & Paul, 2001a, 2001b; Neugebauer et al., 2005; O'Leary & Paul, 2006; Pankaj et al., 2009), long aliphatic hydrocarbon side chains lead to the phenomenon of "side-chain crystallization," i.e., the lateral chains pack into crystallites, even if the backbone of the polymer to which they are attached is not stereoregular. All of carbohydrate polymers under study contain a long side open-chain structure and, in addition, they are amphiphilic, both features favoring the potential of side-chain crystallization. Nevertheless, the content of counit with carbohydrate moieties must be high enough to allow lateral crystallization. These open-saccharide chains would tend to be positioned, more or less, parallel to one another in the crystallites, so that the crystals would have a layer arrangement. Perfection of this crystalline ordering is rather dependent on composition, as seen in Fig. 4a. An increase of MMA content, the non-crystallizable comonomer, affects the final structure of the copolymer in several ways. First, it reduces the overall number of crystallizable chains in the copolymer; second, it interrupts and impedes the crystallizable side chains from forming perfect crystals; and, third, it forces the amorphous backbone to contort to accommodate the side chains crystallizing around the non-crystallizable lateral-chains, which hinders the conformational freedom of the backbone. These effects reduce the overall crystallization capability and, then, the crystallinity as well as T_m and enthalpy are depressed in the carbohydrate copolymers (see Table S2).

Fig. 4b shows that PHEAG exhibits two broad amorphous-like peaks at 150 °C. The main peak is at this temperature higher than the T_m estimated by DSC, indicative of a mostly disordered structure if compared with the pattern displayed at room temperature. These two peaks are centered at 2θ values of 8.8° and 19.2°, i.e., they correspond to spacing values of 1.01 nm and 0.46 nm, respectively. Both peaks behave in a different manner as MMA comonomer content increases in the carbohydrate copolymer. The former one moves to higher angle values while the second peak displaces to slightly lower angles. It has been reported that maximum at the higher angles is related to most probable intermolecular distances within side-chain while the low angle peak refers to those ascribed to main chain contacts (Jones, 1964).

Fig. 4c represents the spacing of the amorphous peak located at around 19° for the various copolymers. It is clearly observed that the most probable intermolecular distance within the lateral chains is closer in the PHEAG homopolymer and increases as MMA content is incorporated and raised in the carbohydrate containing copolymer, indicating a more compact packing in PHEAG even in the isotropic state probably due to the higher number of hydrogen bonds existing within its architecture.

Fig. 6 depicts the results obtained in the variable-temperature WAXS experiments. The crystalline ordering is rather imperfect even in PHEAG and, then, no clear diffraction peaks are seen. This fact might be associated with the inherent chemical composition heterogeneity in these amphiphilic materials under evaluation. Nevertheless, some similarities are deduced from the analysis of these profiles for PHEAG and for P(M*x*G*y*) copolymers with $F_{HEAG} \geq 0.5$. They basically consist of an improvement in the ordered arrangements at temperatures ranging 40–70 °C, followed by the beginning of the melting of the smallest entities and the primary melting process at higher temperatures. Therefore, T_m can be determined and the values obtained are represented in Fig. S5 comparing them with those obtained from conventional DSC and SAXS measurements. It can be seen that the agreement between the T_m estimated from these three complementary techniques is rather good.
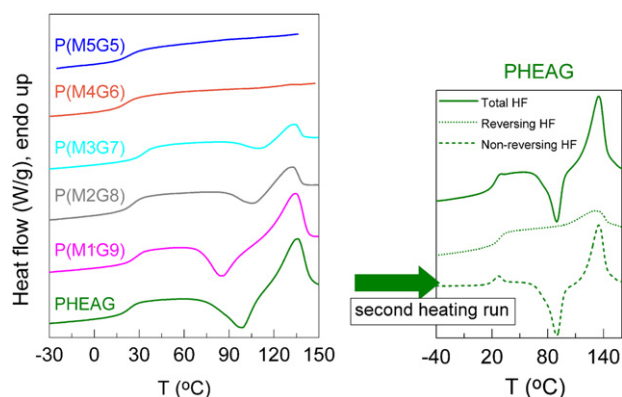
Fig. 7. DSC curves on heating after a fast cooling process in the calorimeter for the P(M*x*G*y*) carbohydrate copolymers with $F_{HEAG} \geq 0.5$ and the PHEAG. In the inset, the MDSC traces (total, reversing and non-reversing HF) are represented for PHEAG on heating after a fast cooling process.

Once the isotropic state is reached in those specimens with an ordering capability, it is very interesting to evaluate the second heating runs after applying a fast cooling to the samples. Fig. 7 displays that crystallization capability in the copolymers with F_{HEAG} equal or higher than 0.5 is rather limited at high cooling rate. Only the PHEAG homopolymer is able to undergo a small ordering during the cooling experiment but in a small amount (see modulated results for the second heating run in the inset). Its main arrangement takes place during its cold crystallization on heating. This feature is easily deduced from the small endothermic peak observed in the reversing component, which is ascribed to the fraction organized during cooling, as well as from the relatively intense glass transition, which is a consequence of its low crystallinity. The kinetic processes that occur on this second heating experiment are seen in the non-reversing response, i.e., the cold crystallization and its subsequent melting. The enthalpic balance from above T_g to the end of this second heating experiment is zero for the P(M1G9), P(M2G8), P(M3G7) and P(M4G6) samples, fact that indicates that crystallization does not happen during cooling and it is only possible to occur on heating. On the other hand, P(M5G5) copolymer become completely amorphous and incapable of self-assembling within this time window.

Moreover, SAXS experiments were performed in order to attain additional information about the crystalline details exhibited by these carbohydrate polymers. Fig. S6 shows the summary from these variable-temperature melting experiments with synchrotron radiation. Fig. S6a depicts that no clear long spacing is observed at any temperature, although the relative SAXS invariant (Baltá-Calleja & Vonk, 1989; Ryan, Stanford, Bras, & Nye, 1997) represented for all of them in Fig. S6b shows a noticeable discontinuity during the melting of the sample. Their derivatives (Fig. S6c) allow determining the melting temperature. Since no long spacing is observed, it seems to indicate that the main chain does not participate in the ordering arising from the lateral crystallization.

3.3. Thermal stability

The knowledge of thermal stability of these novel carbohydrate polymeric materials is quite important in order to evaluate their final applicability. Fig. 8 shows the thermogravimetric (TG) and derivative thermogravimetric (DTG) curves of these P(HEAG-MMA) carbohydrate copolymers (results collected in Table S3). The copolymers under study are rather hydrophilic since contain saccharides with open-chain structures that are more hygroscopic than those with cyclic architectures. In order to avoid an overlapping of this water loss with an actual degradation stage
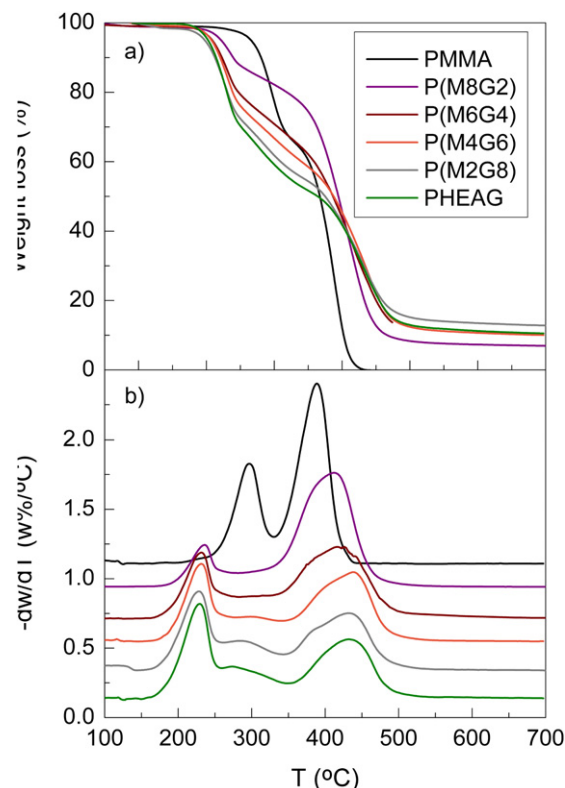

Fig. 8. (a) TG and (b) DTG curves for PMMA and PHEAG and P(M*x*G*y*) carbohydrate copolymers under inert environment. DTG curves have been vertically shifted for clarity.

that might occur at the same temperature range and lose some important piece of information, copolymers were dried immediately before the thermogravimetric measurements. Accordingly, the initial stage located between 100 and 160 °C and ascribed to loss of adsorbed and absorbed water (Athawale & Lele, 2000; Cerrada, Sanchez-Chaves, et al., 2009; Cerrada, Sanchez-Chaves, Ruiz, & Fernandez-Garcia, 2010; Don & Chen, 2005; Lanthong, Nuisin, & Kiatkamjornwong, 2006; Ruiz, Sanchez-Chaves, Cerrada, & Fernandez-Garcia, 2008; Stewart, Harrup, Lash, & Tsang, 2000) characteristic, particularly, in carbohydrate copolymers and, in general, in polysaccharides is not observed.

Degradation takes place through three clear weight losses in all the copolymers. The first and second stages are almost consecutives and are assigned to the decomposition of carbohydrate groups involving water and carbon dioxide formation (Cerrada, Ruiz, Sanchez-Chaves, & Fernandez-Garcia, 2009). The last stage is associated with the remaining macromolecular chain degradation.

It is evident that independently of HEAG composition in the statistical copolymer, the degradation temperatures of the different stages are quite similar, although these temperatures are always higher than those of PHEAG. In addition, the mass loss corresponding to the different stages is definitely dependent on composition. The ratio of first and second stages decreases as HEAG composition. Experimental and theoretical values of both two stages are listed in Table S3 and a good agreement is found. This feature confirms that the carbohydrate copolymers are obtained at high conversion, near 100%, and consequently, their final copolymer composition is practically the initial used in the feed, $F_{final,i} \cong f_{initial,i}$.

4. Conclusions

Amphiphilic carbohydrate polymers containing long side-chains have been obtained by free radical copolymerization of

unprotected glycomonomer and methyl methacrylate. The in situ copolymerization reactions performed in glass tube and followed by ^{1}H NMR have allowed obtaining the copolymer composition in the feed and in the copolymer through the whole conversion. Consequently, the kinetic behavior and the monomer reactivity reactions have been calculated, pointing out that the reactivity of methyl methacrylate radical against HEAG is lower than against MMA, whereas HEAG radical reacts rather with MMA than with its glycomonomer. To study the properties of these carbohydrate copolymers, copolymerization reactions at very high conversion have been performed with compositions ranging from 0.1 to 0.9. The existence of ordering in carbohydrate copolymers with HEAG compositions equal or higher than 0.5 has been demonstrated by conventional and modulated differential scanning calorimetry as well as by X-ray diffraction measurements. At the same time, the phase separation behavior of the copolymers with compositions HEAG lower than 0.5 has revealed the existence of two glass transitions attributed to the main and the side chains. Finally, the thermal stability of all these amphiphilic copolymers has been evaluated by thermogravimetric analysis, establishing the relationship between the structure and properties.

Acknowledgments

Appendix A. Supplementary data

Supplementary data associated with this article can be found, in the online version, at http://dx.doi.org/10.1016/j.carbpol.2013.01.053.

References

Athawale, V. D., & Lele, V. (2000). Thermal studies on granular maize starch and its graft copolymers with vinyl monomers. *Starch – Stärke*, 52(6–7), 205–213.

Bahulekar, R., Tokiwa, T., Kano, J., Matsumura, T., Kojima, I., & Kodama, M. (1998). Polyacrylamide containing sugar residues: Synthesis, characterization and cell compatibility studies. *Carbohydrate Polymers*, 37(1), 71–78.

Baltá-Calleja, F. J., & Vonk, C. G. (1989). *X-ray scattering of synthetic polymers*. Amsterdam, Netherlands: Elsevier.

Beiner, M. (2001). Relaxation in poly(alkyl methacrylate)s: Crossover region and nanophase separation. *Macromolecular Rapid Communications*, 22(12), 869–895.

Bertozzi, C. R., & Kiessling, L. L. (2001). Chemical glycobiology. *Science*, 291(5512), 2357–2364.

Bordege, V., Munoz-Bonilla, A., Leon, O., Cuervo-Rodriguez, R., Sanchez-Chaves, M., & Fernandez-Garcia, M. (2011). Gluconolactone-derived polymers: Copolymerization, thermal properties, and their potential use as polymeric surfactants. *Journal of Polymer Science Part A: Polymer Chemistry*, 49(2), 526–536.

Bordegé, V., Muñoz-Bonilla, A., León, O., Sánchez-Chaves, M., Cuervo-Rodríguez, R., & Fernández-García, M. (2011). Glycopolymers with glucosamine pendant groups: Copolymerization, physico-chemical and interaction properties. *Reactive and Functional Polymers*, 71(1), 1–10.

Cameron, N. R., Spain, S. G., Kingham, J. A., Weck, S., Albertin, L., Barker, C. A., et al. (2008). Synthesis of well-defined glycopolymers and some studies of their aqueous solution behaviour. *Faraday Discussions*, 139, 359–368.

Cerrada, M. L., Ruiz, C., Sanchez-Chaves, M., & Fernandez-Garcia, M. (2009). Molecular recognition capability and rheological behavior in solution of novel lactone-based glycopolymers. *European Polymer Journal*, 45(11), 3176–3184.

Cerrada, M. L., Sanchez-Chaves, M., Ruiz, C., & Fernandez-Garcia, M. (2009). Recognition abilities and development of heat-induced entangled networks in lactone-derived glycopolymers obtained from ethylene-vinyl alcohol copolymers. *Biomacromolecules*, 10(7), 1828–1837.

Cerrada, M. L., Sanchez-Chaves, M., Ruiz, C., & Fernandez-Garcia, M. (2010). Specific lectin interactions and temperature-induced reversible gels in novel water-soluble glycopolymers bearing maltotrionolactone pendant groups. *Journal of Polymer Science Part A: Polymer Chemistry*, 48(3), 719–729.

Coote, M. L., & Davis, T. P. (1999). The mechanism of the propagation step in free-radical copolymerisation. *Progress in Polymer Science*, 24(9), 1217–1251.

Cowie, J. M. G., Haq, Z., McEwen, I. J., & Velićkovič, J. (1981). Poly(alkyl itaconates): 8. Observations of dual glass transitions and crystallinity in the dialkyl ester series diheptyl to di-eicosyl. *Polymer*, 22(3), 327–332.

Chen, X., Dordick, J. S., & Rethwisch, D. G. (1995). Chemoenzymic synthesis and characterization of poly(α-methyl galactoside 6-acrylate) hydrogels. *Macromolecules*, 28(18), 6014–6019.

Chen, W., & Wunderlich, B. (1999). Nanophase separation of small and large molecules. *Macromolecular Chemistry and Physics*, 200(2), 283–311.

de la Fuente, J. L., Fernandez-Garcia, M., Cerrada, M. L., Spiess, H. W., & Wilhelm, M. (2006). Small-angle X-ray scattering and linear melt rheology of poly(tert-butyl acrylate-g-styrene) graft copolymers. *Polymer*, 47(5), 1487–1495.

Don, T.-M., & Chen, H.-R. (2005). Synthesis and characterization of AB-crosslinked graft copolymers based on maleilated chitosan and N-isopropylacrylamide. *Carbohydrate Polymers*, 61(3), 334–347.

Feijoo, J. L., Muller, A. J., & Acosta, J. R. (1986). A study on the compatibility of poly(methyl methacrylate) methyl-methacrylate styrene random copolymer blends. *Journal of Materials Science Letters*, 5(3), 313–314.

Fernandez-Garcia, M., Cuervo-Rodriguez, R., & Madruga, E. L. (1999). Glass transition temperatures of butyl acrylate-methyl methacrylate copolymers. *Journal of Polymer Science Part B: Polymer Physics*, 37(17), 2512–2520.

Fernandez-Garcia, M., Lopez-Gonzalez, M. M. C., Barrales-Rienda, J. M., Madruga, E. L., & Arias, C. (1994). Effect of copolymer composition and conversion on the glass-transition of methyl acrylate-methyl methacrylate copolymers. *Journal of Polymer Science Part B: Polymer Physics*, 32(7), 1191–1203.

Fukuda, T., Goto, A., Kwak, Y., Yoshikawa, C., & Ma, Y. D. (2002). Penultimate unit effects in free radical copolymerization. *Macromolecular Symposia*, 182, 53–64.

García-Oteiza, M. C., Sánchez-Chaves, M., & Arranz, F. (1997). Poly(vinyl alcohol) having amino sugar as the pendant group: Synthesis, characterization and binding of concanavalin A. *Macromolecular Chemistry and Physics*, 198(7), 2237–2247.

Gauthier, M. A., Gibson, M. I., & Klok, H.-A. (2009). Synthesis of functional polymers by post-polymerization modification. *Angewandte Chemie International Edition*, 48(1), 48–58.

Gómez Tejedor, J. A., Rodríguez Hernández, J. C., Gómez Ribelles, J. L., & Monleón Pradas, M. (2007). Dynamic mechanical relaxation of poly(2-hydroxyethyl acrylate)-silica nanocomposites obtained by the sol–gel method. *Journal of Macromolecular Science, Part B*, 46(1), 43–54.

Hadjichristidis, N., Pispas, S., & Floudas, G. (2003). Nonlinear block copolymers. In *Block copolymers*. Hoboken, New Jersey: John Wiley & Sons, Inc. (pp. 126–172)

Höhne, G. W. H. (1999). Temperature modulated differential scanning calorimetry (TMDSC) in the region of phase transitions. Part 1: theoretical considerations. *Thermochimica Acta*, 330(1–2), 45–54.

Jones, A. T. (1964). Crystallinity in isotactic polyolefins with unbranched side chains. *Die Makromolekulare Chemie*, 71(1), 1–32.

Jordan, E. F. (1971). Side-chain crystallinity. III. Influence of side-chain crystallinity on the glass transition temperatures of selected copolymers incorporating *n*-octadecyl acrylate or vinyl stearate. *Journal of Polymer Science Part A: Polymer Chemistry*, 9(11), 3367–3378.

Jordan, E. F., Artymyshyn, B., Speca, A., & Wrigley, A. N. (1971). Side-chain crystallinity. II. Heats of fusion and melting transitions on selected copolymers incorporating *n*-octadecyl acrylate or vinyl stearate. *Journal of Polymer Science Part A: Polymer Chemistry*, 9(11), 3349–3365.

Karaky, K., Clisson, G., Reiter, G., & Billon, L. (2008). Semicrystalline macromolecular design by nitroxide-mediated polymerization. *Macromolecular Chemistry and Physics*, 209(7), 715–722.

Karamuk, E., Mayer, J., Wintermantel, E., & Akaike, T. (1999). Partially degradable film/fabric composites: Textile scaffolds for liver cell culture. *Artificial Organs*, 23(9), 881–884.

Kiessling, L. L., Gestwicki, J. E., & Strong, L. E. (2006). Synthetic multivalent ligands as probes of signal transduction. *Angewandte Chemie International Edition*, 45(15), 2348–2368.

Kobayashi, K., Tsuchida, A., Usui, T., & Akaike, T. (1997). A new type of artificial glycoconjugate polymer: A convenient synthesis and its interaction with lectins. *Macromolecules*, 30(7), 2016–2020.

Ladmiral, V., Melia, E., & Haddleton, D. M. (2004). Synthetic glycopolymers: An overview. *European Polymer Journal*, 40(3), 431–449.

Lanthong, P., Nuisin, R., & Kiatkamjornwong, S. (2006). Graft copolymerization, characterization, and degradation of cassava starch-g-acrylamide/itaconic acid superabsorbents. *Carbohydrate Polymers*, 66(2), 229–245.

Lee, C., Gido, S. P., Pitsikalis, M., Mays, J. W., Tan, N. B., Trevino, S. F., et al. (1997). Asymmetric single graft block copolymers: Effect of molecular architecture on morphology. *Macromolecules*, 30(13), 3732–3738.

López-Velázquez, D., Bello, A., & Pérez, E. (2004). Preparation and characterisation of hydrophobically modified hydroxypropylcellulose: Side-chain crystallisation. *Macromolecular Chemistry and Physics*, 205(14), 1886–1892.

Mammen, M., Choi, S.-K., & Whitesides, G. M. (1998). Polyvalent interactions in biological systems: Implications for design and use of multivalent ligands and inhibitors. *Angewandte Chemie International Edition*, 37(20), 2754–2794.

Matsushita, Y., & Noda, I. (1996). Morphology and domain size of a model graft copolymer. *Macromolecular Symposia*, 106(1), 251–257.

Mayo, F. R., & Lewis, F. M. (1944). Copolymerization I A basis for comparing the behavior of monomers in copolymerization, the copolymerization of styrene and methyl methacrylate. *Journal of the American Chemical Society*, 66, 1594–1601.

McKenzie, B. E., Nudelman, F., Bomans, P. H. H., Holder, S. J., & Sommerdijk, N. A. J. M. (2010). Temperature-responsive nanospheres with bicontinuous internal structures from a semicrystalline amphiphilic block copolymer. *Journal of the American Chemical Society*, *132*(30), 10256–10259.

Mogri, Z., & Paul, D. R. (2001a). Gas sorption and transport in poly(alkyl (meth)acrylate)s. II. Sorption and diffusion properties. *Polymer*, *42*(18), 7781–7789.

Mogri, Z., & Paul, D. R. (2001b). Water-vapor permeation in semicrystalline and molten poly(octadecyl acrylate). *Journal of Polymer Science Part B: Polymer Physics*, *39*(10), 979–984.

Mun, G. A., Khutoryanskiy, V. V., Akhmetkalieva, G. T., Shmakov, S. N., Dubolazov, A. V., Nurkeeva, Z. S., et al. (2004). Interpolymer complexes of poly(acrylic acid) with poly(2-hydroxyethyl acrylate) in aqueous solutions. *Colloid and Polymer Science*, *283*(2), 174–181.

Munoz-Bonilla, A., Cerrada, M. L., & Fernandez-Garcia, M. (2007a). Physical properties of poly(cyclohexyl methacrylate)-b-poly(iso-butyl acrylate)-b-poly(cyclohexyl methacrylate) triblock copolymers synthesized by controlled radical polymerization. *Polymer*, *48*(19), 5581–5589.

Munoz-Bonilla, A., Cerrada, M. L., & Fernandez-Garcia, M. (2007b). Self-assembly of ATRP-synthesized PCH-b-PtBA-b-PCH triblock copolymers observed by time-resolved SAXS. *Macromolecular Chemistry and Physics*, *208*(24), 2654–2664.

Munoz-Bonilla, A., Fernandez-Garcia, M., Cerrada, M. L., Mantovani, G., & Haddleton, D. M. (2007). Aggregation and solubilization of organic solvents and petrol/gasoline in water mediated by block copolymers. *European Polymer Journal*, *43*(11), 4583–4592.

Munoz-Bonilla, A., Fernandez-Garcia, M., & Haddleton, D. M. (2007). Synthesis and aqueous solution properties of stimuli-responsive triblock copolymers. *Soft Matter*, *3*(6), 725–731.

Muñoz-Bonilla, A., León, O., Cerrada, M. L., Rodríguez-Hernández, J., Sánchez-Chaves, M., & Fernández-García, M. (2012). Glycopolymers obtained by chemical modification of well-defined block copolymers. *Journal of Polymer Science Part A: Polymer Chemistry*, *50*(13), 2565–2577.

Neugebauer, D., Theis, M., Pakula, T., Wegner, G., & Matyjaszewski, K. (2005). Densely heterografted brush macromolecules with crystallizable grafts. Synthesis and bulk properties. *Macromolecules*, *39*(2), 584–593.

O'Leary, K. A., & Paul, D. R. (2006). Physical properties of poly(*n*-alkyl acrylate) copolymers. Part 2. Crystalline/non-crystalline combinations. *Polymer*, *47*(4), 1245–1258.

Okada, M. (2001). Molecular design and syntheses of glycopolymers. *Progress in Polymer Science*, *26*(1), 67–104.

Pankaj, S., Hempel, E., & Beiner, M. (2009). Side-chain dynamics and crystallization in a series of regiorandom poly(3-alkylthiophenes). *Macromolecules*, *42*(3), 716–724.

Polikarpov, N., Kaufmann, A., Kluge, J., Appelhans, D., & Voit, B. (2010). Investigation of dye glycopolymer and glycopolymer hydrogel interactions for development of multi-release system. *Journal of Controlled Release*, *148*(1), e66–e67.

Reading, M., Luget, A., & Wilson, R. (1994). Modulated differential scanning calorimetry. *Thermochimica Acta*, *238*, 295–307.

Ruiz, C., Sanchez-Chaves, M., Cerrada, M. L., & Fernandez-Garcia, M. (2008). Glycopolymers resulting from ethylene-vinyl alcohol copolymers: Synthetic approach, characterization, and interactions with lectins. *Journal of Polymer Science Part A: Polymer Chemistry*, *46*(21), 7238–7248.

Ryan, A. J., Stanford, J. L., Bras, W., & Nye, T. M. W. (1997). A synchrotron X-ray study of melting and recrystallization in isotactic polypropylene. *Polymer*, *38*(4), 759–768.

Simon, S. L. (2001). Temperature-modulated differential scanning calorimetry: Theory and application. *Thermochimica Acta*, *374*(1), 55–71.

Spain, S. G., & Cameron, N. R. (2011). A spoonful of sugar: The application of glycopolymers in therapeutics. *Polymer Chemistry*, *2*(1), 60–68.

Spain, S. G., Gibson, M. I., & Cameron, N. R. (2007). Recent advances in the synthesis of well-defined glycopolymers. *Journal of Polymer Science Part A: Polymer Chemistry*, *45*(11), 2059–2072.

Stewart, F. F., Harrup, M. K., Lash, R. P., & Tsang, M. N. (2000). Synthesis, characterization and thermal stability of phosphazene terpolymers with 2-(2-methoxyethoxy)ethoxy and diacetone D-glucofuranosyl pendant groups. *Polymer International*, *49*(1), 57–62.

Stickler, M. (1987). Experimental-techniques in free-radical polymerization kinetics. *Makromolekulare Chemie-Macromolecular Symposia*, *10*, 17–69.

Teng, H., Koike, K., Zhou, D., Satoh, Z., Koike, Y., & Okamoto, Y. (2009). High glass transition temperatures of poly(methyl methacrylate) prepared by free radical initiators. *Journal of Polymer Science Part A: Polymer Chemistry*, *47*(1), 315–317.

Ting, S. R. S., Chen, G., & Stenzel, M. H. (2010). Synthesis of glycopolymers and their multivalent recognitions with lectins. *Polymer Chemistry*, *1*(9), 1392–1412.

Top, A., & Kiick, K. L. (2010). Multivalent protein polymers with controlled chemical and physical properties. *Advanced Drug Delivery Reviews*, *62*(15), 1530–1540.

Tudos, F., Kelen, T., Foldesberezsnich, T., & Turcsanyi, B. (1976). Analysis of linear methods for determining copolymerization reactivity ratios. 3. Linear graphic method for evaluating data obtained at high conversion levels. *Journal of Macromolecular Science – Chemistry, A*, *10*(8), 1513–1540.

Varma, A. J., Kennedy, J. F., & Galgali, P. (2004). Synthetic polymers functionalized by carbohydrates: A review. *Carbohydrate Polymers*, *56*(4), 429–445.

Wunderlich, B. (1997). Modeling the heat flow and heat capacity of modulated differential scanning calorimetry. *Journal of Thermal Analysis and Calorimetry*, *48*(2), 207–224.

Wunderlich, B., Boller, A., Okazaki, I., Ishikiriyama, K., Chen, W., Pyda, M., et al. (1999). Temperature-modulated differential scanning calorimetry of reversible and irreversible first-order transitions. *Thermochimica Acta*, *330*(1–2), 21–38.

Xu, Z., Wan, L., & Huang, X. (2009). Membranes with glycosylated surface. In *Surface engineering of polymer membranes*. Berlin Heidelberg: Springer. (pp. 202–224).

Yang, Q., Xu, Z.-K., Dai, Z.-W., Wang, J.-L., & Ulbricht, M. (2005). Surface modification of polypropylene microporous membranes with a novel glycopolymer. *Chemistry of Materials*, *17*(11), 3050–3058.

Zhou, W.-J., Kurth, M. J., Hsieh, Y.-L., & Krochta, J. M. (1999). Synthesis and thermal properties of a novel lactose-containing poly(N-isopropylacrylamide-co-acrylamidolactamine) hydrogel. *Journal of Polymer Science Part A: Polymer Chemistry*, *37*(10), 1393–1402.